

Article

LED Current Balance Using a Variable Voltage Regulator with Low Dropout v_{DS} Control

Hung-I Hsieh * and Hao Wang

Department of Electrical Engineering, National Chiayi University; Chiayi City 60004, Taiwan; hsieh.henry2@gmail.com

* Correspondence: hihsieh@mail.ncyu.edu.tw; Tel.: +886-5-2717-981

Academic Editor: Eric Ka-wai Cheng

Received: 26 December 2016; Accepted: 14 February 2017; Published: 20 February 2017

Abstract: A cost-effective light-emitting diode (LED) current balance strategy using a variable voltage regulator (VVR) with low dropout v_{DS} control is proposed. This can regulate the multiple metal-oxide-semiconductor field-effect transistors (MOSFETs) of the linear current regulators (LCR), maintaining low dropout v_{DS} on the flat v_{GS} -characteristic curves and making all drain currents almost the same. Simple group LCRs respectively loaded with a string LED are employed to implement the theme. The voltage VV_{dc} from a VVR is synthesized by a string LED voltage Nv_D , source voltage v_R , and a specified low dropout $v_{DS} = V_Q$. The VV_{dc} updates instantly, through the control loop of the master LCR, which means that all slave MOSFETs have almost the same biases on their flat v_{GS} -characteristic curves. This leads to all of the string LED currents being equal to each other, producing an almost even luminance. An experimental setup with microchip control is built to verify the estimations. Experimental results show that the luminance of all of the string LEDs are almost equal to one another, with a maximum deviation below 1% during a wide dimming range, while keeping all v_{DS} of the MOSFETs at a low dropout voltage, as expected.

Keywords: linear current regulator; variable voltage regulator; LED; low dropout voltage

1. Introduction

The improving of lighting efficiency is one of the direct ways to contribute to energy-saving and green environment initiatives. Furthermore, mercury-free requests for avoiding the release of pollution into the environment also form part of the vital work at present. Accordingly, light-emitting diodes (LEDs) have become the necessary option in the lighting environmental renovation. Even the power LED has advantages, including a high-fidelity, high rendering, and low power consumption. Currently, the most urgent task is to understand how to make LED luminance become a surface light source, such as a fluorescent lamp. The most effective way to do this is by using a much lower-power LED to implement the surface source. To date, effective control strategies for balancing LED currents only include the linear balancing way and the digital pulse balancing way, such as is shown in Figure 1 [1–10]; in which Figure 1a,b demonstrate linear balancing ways and Figure 1c illustrates the digital pulse balancing way. In Figure 1a, all LED strings are supplied by a constant voltage source (CVS). In this situation, the LED current balance can be easily determined by a voltage detected from a sense resistor. However, this technique may cause a sense voltage change, especially for the CVS supply, since the LED forward voltage will vary with the ambient temperature [11]. As shown in Figure 1b, a shunt current balance configuration is built with a constant current source (CCS) supply, in which all of the string LED currents are collected into the controller and then individually compared with the reference current. This can achieve more accurate current balancing between adjacent LEDs, in order to emit uniform light. In Figure 1c, a digital pulse shunt current balance circuit is implemented with a supply of either voltage source (VS) or current source (CS). In this case,

LED current balancing mainly uses a PWM duty cycle control, such as sequential phase-shift duty control [12,13], burst mode [14,15], self-adaptive control [16], and series-connected mode [17], etc. In this case, the LED driven by the pulse to emit luminance for a human is based on the persistence of vision. Although the LED current balance by pulse drives can be conducted by multiplexing, it is difficult to make all of the string LED currents balanced for obtaining a uniform light source. To improve this problem, the luminance's area should be fed back to adjust the adjacent string currents, producing a uniform light source. In spite of the fact that the mentioned current balance strategies are available, an uncertainty of the balance between the adjacent string LEDs always exists, mainly due to temperature variation and the dimming process. Further, the cost-effective way to perform a large scale lighting display is by using a shunt current balance configuration by linear current regulators (LCR) with a single voltage source [13,18]. Above all, the MOSFET of LCR may dissipate more conduction loss, due to an uncertain drain-to-source voltage on the i_{DS} - v_{DS} plane [19]. Besides, many balance cells for LEDs directly using versatile dc/dc converters or resonant converters have been successively developed [18,20–25]. However, in terms of application for a large scale display, it is difficult to implement a large lighting area using such a large amount LED cells, needed to acquire a balanced luminance. In fact, the cost-effective way to perform a large scale lighting display is to use multiple shunt current balance configurations, controlled by multiple linear current regulators (LCR) with only a single voltage source. In this paper, to improve the characteristics of LCRs for driving the string LEDs, all operation points of the MOSFETs are separately placed on their v_{GS} -controlled characteristic curves; curves which are produced from an array of IC values and which are expected to present correspondingly similar results [19]. On the specified almost-equal saturation-level curves, all string LEDs are then driven by almost constant drain currents to produce an equal luminance, even though the v_{DS} 's are scattered under the curves. Successively, an approach to place all MOSFET v_{DS} with a low dropout voltage on the specified flat curve in the saturation region is revealed [26]. Accordingly, a variable voltage regulator (VVR) is then proposed to perform the idea, such that all MOSFETs operate on the specified flat saturation curve with low dropout v_{DS} . The output voltage VV_{dc} of the VVR is synthesized by a string voltage Nv_D of N -LED, detected source voltage v_R , and a specified low dropout $v_{DS} = V_Q$. With the supply of VV_{dc} to LCRs, all string LEDs can be biased at almost the same saturation-level curves, respectively, whose currents will then be almost equal and can excite all string LEDs to produce an almost even luminance. Modeling the multiple LCRs for regulating constant string currents is conducted. An experimental setup for assessing the control strategies of balancing the multiple string LEDs is built. An aspect of the LCR for the string LED drives is described in Section 2. Using a variable voltage regulator (VVR) as the LCR supply, to excite the string LEDs for the production of a current balance, is explored in Section 3. The design and experiment for verifying the predicted estimations is discussed in Section 4. Final comments are concluded in Section 5.

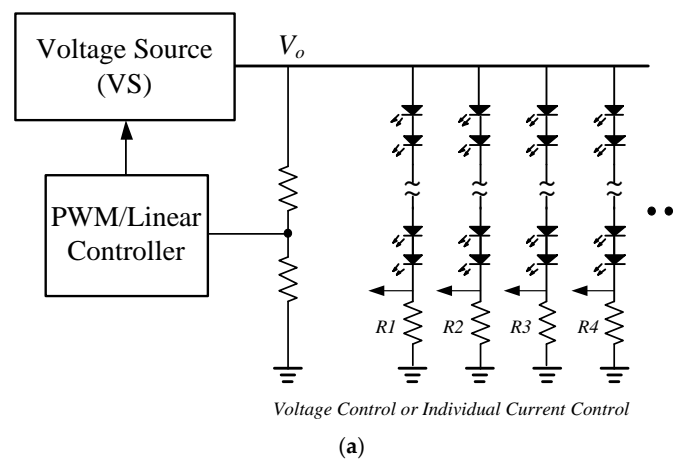


Figure 1. Cont.

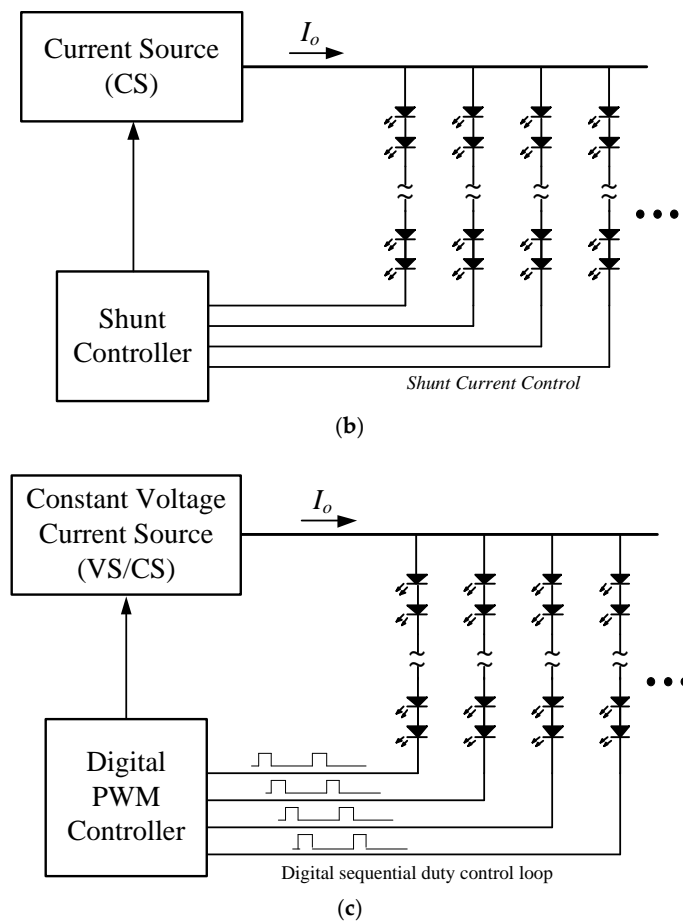


Figure 1. Commonly-used LED drives: (a) Voltage control or individual current control by constant voltage source supply; (b) Shunt current control with current source supply; (c) Digital PWM duty control using shunt current balance.

2. Aspect of Linear Current Regulator for LEDs

2.1. Linear Current Regulator

Figure 2a shows the commonly-used LCR, which is a current-series feedback configuration composed of a MOSFET, an operational amplifier (OPA), and a sense resistor R_s . A string LED is widely loaded on the MOSFET in application. We define the symbols herein such that $v_{DS} = V_{DS} + v_{ds}$, where v_{DS} is for the total signal, V_{DS} is the dc component, and v_{ds} is the small signal. The small-signal model of the LCD is depicted in Figure 2b, in which the output current (drain current of MOSFET) i_{DS} is given by [17]. If $A_v \gg 1$ and $g_m A_v R_s \gg 1$, this yields:

$$i_{DS} \cong \frac{V_+}{R_s}, \tag{1}$$

Presuming that the MOSFET operates in the saturation region, i_{DS} in (1) is almost a constant current, varying with the input voltage V_+ . This drain current can also be directly found from the characteristic curve of the MOSFET, guided by a certain v_{GS} .

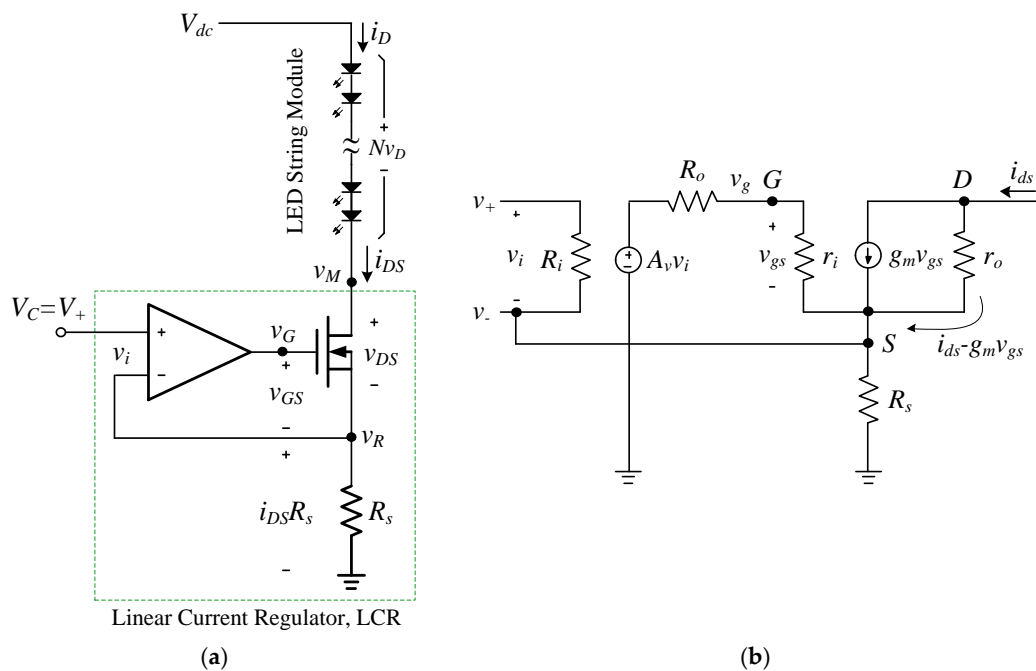


Figure 2. (a) Typical linear current regulator (LCR) loaded with a string LED; (b) Small-signal model of the LCR.

2.2. LED String Module in LCR

Bias Situation for a Single String LED

An LED is essentially a family of diodes, whose current is temperature-dependent and varies, approximately in exponential form, in its forward bias [19]. The relation of the general LED current i_D and the voltage v_D can be simply expressed by the Shockley equation; for a single LED, this is presented as:

$$i_D(v_D) = I_s(e^{\frac{v_D}{\eta V_T}} - 1), \tag{2}$$

and

$$v(i_D) = v(i_{DS}) = \eta V_T \ln\left(\frac{i_{DS} + I_s}{I_s}\right), \tag{3}$$

where I_s is the leakage current in reverse bias, V_T is the thermal voltage, η is the ideality factor, v_D is the forward voltage, and v_{DS} is the drain-to-source voltage of MOSFET. For a number of N LEDs connected in a series to form the string N -LED, the voltage v_{DN} of the forward bias can be given by:

$$\begin{aligned} v_{DN} &\equiv Nv_D = \eta N V_T \ln\left(\frac{i_{DS} + I_s}{I_s}\right) \\ &= \eta N V_T \ln\left(\frac{i_{DS} + I_s}{I_s}\right) \end{aligned} \tag{4}$$

where $i_{DS} = i_D$ is due to the series connection of N -LED, and N is an integer. With the assumption of the diode ideality factor $\eta = 1$ in standard fabrication, and if $i_D \gg I_s$, we can simplify Equation (4) as:

$$\begin{aligned} v_{DN} &\approx N V_T \ln\left(\frac{i_D}{I_s}\right) \\ &\approx N V_T \ln\left(\frac{i_{DS}}{I_s}\right) \end{aligned} \tag{5}$$

In Figure 2a, the loop equation for the LCR loaded with the string N -LED can be given by:

$$V_{dc} = v_{DS} + Nv_D + i_{DS}R_s, \tag{6}$$

where V_{dc} is the dc supply voltage. The drain-to-source voltage of the MOSFET can be given by:

$$\begin{aligned} v_{DS} &= V_{dc} - Nv_D - i_{DS}R_s \\ &= V_{dc} - v \end{aligned} \tag{7}$$

where we let v be the voltage sum, i.e.,

$$v = Nv_D + i_{DS}R_s, \tag{8}$$

Form (6), the drain current of the MOSFET in the LCR can also be given by

$$\begin{aligned} i_{DS} &= f(v_{DS}) \\ &= \frac{1}{R_s}(V_{dc} - Nv_D - v_{DS}) \end{aligned} \tag{9}$$

For the convenience of analysis, point M is set to measure the drain voltage of the MOSFET, v_M , and Equation (6) can then be modified as:

$$\begin{aligned} v_M &= V_{dc} - Nv_D \\ &= v_{DS} + i_{DS}R_s \end{aligned} \tag{10}$$

If a small variation of v_D is neglected, V_M instead of v_M is given by:

$$\begin{aligned} V_M &= V_{dc} - NV_D \\ &= V_{DS} + I_{DS}R_s \end{aligned} \tag{11}$$

Equation (11) represents a LCR loaded with one string N -LEDs and supplied by a voltage $V_M = V_{dc} - NV_D$. The combined characteristics of the one string N -LED and MOSFET of the LCR for bias and load-line descriptions, is shown in Figure 3a.

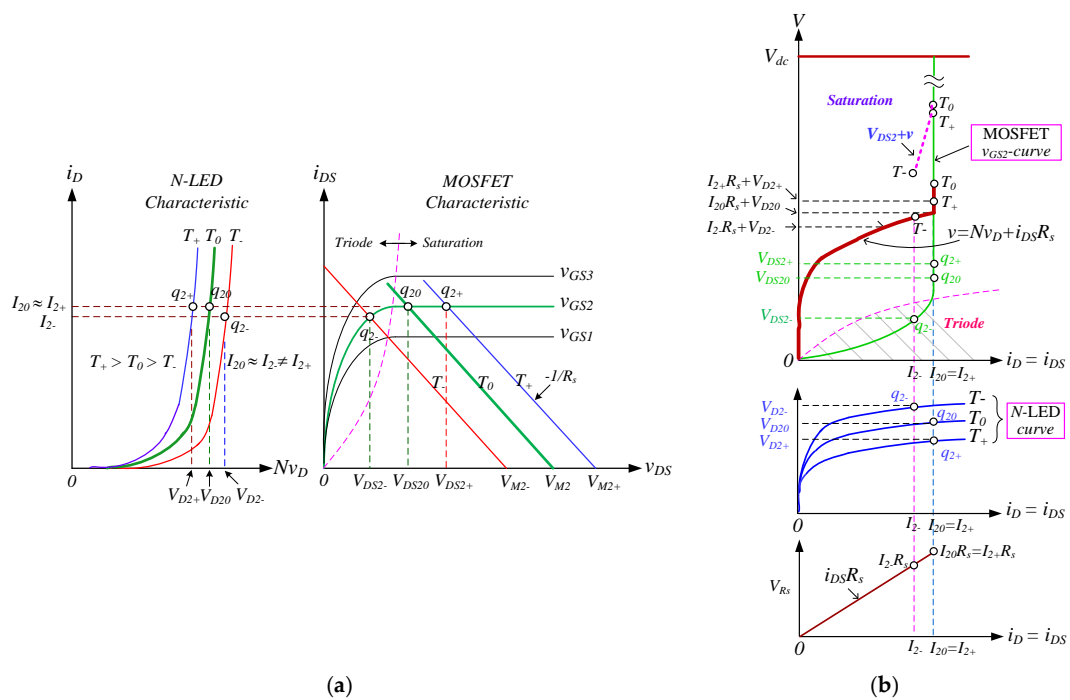


Figure 3. Predicted bias situation of a LCR loaded with one string N -LEDs by a constant voltage V_{dc} supply: (a) Combined characteristics of the one string N -LED and MOSFET of a LCR for bias and load-line descriptions; (b) Bias situation of the LCR for $T_+ > T_0 > T_-$.

In this study, only the three kinds of temperature variations $T_+ > T_0 > T_-$ for the string N -LED are considered. Because of temperature-dependence, the voltage change of the N -LED will lead to a change in V_M , resulting in a move of the load line of MOSFET on the i_{DS} - v_{DS} plane, which is clearly explored in Figure 3a. Correspondingly, the characteristics of N -LED on the i_D - v_D plane for the mentioned temperature variation are also depicted. In addition, the bias situation in the LCR with a constant V_{dc} supply is predictively shown in Figure 3b under temperature variation $T_+ > T_0 > T_-$, including the sense voltage $v_{Rs} = i_{DS}R_s$, Nv_D , v_{DS} , and the voltage sum v etc., all are presented with respect to the current $i_{DS} = i_D$.

(1) Ambient Temperature at $T = T_0$

In this situation, $T = T_0$, we presume that the MOSFET is initially biased at v_{GS2} . A thick-green dc load line of the MOSFET on the i_{DS} - v_{DS} plane is presented by (11), and the corresponding string N -LED characteristic curve on the i_D - v_D plane is given by (2), as respectively shown in Figure 3a. In other words, the operation point of MOSFET is at (I_{DS20}, V_{DS20}) and that of the N -LEDs is at (I_{D20}, V_{D0}) , where $I_{DS20} = I_{D20}$, while we presume that the point q_{20} has a low dropout voltage V_{DS20} . For the load line on the i_{DS} - v_{DS} plane in this situation, the supply to the drain of the MOSFET is equivalent to V_{M2} under the gate drive of v_{GS2} in (11) and the $V_{DS2} = (V_{M2} - V_{Rs})$.

(2) Temperature falling to $T = T_-$

Once the environmental temperature T falls to T_- from T_0 , where $T_- < T_0$, the string N -LED voltage will increase to $V_{D2} = Nv_{D-}$, due to the negative temperature-dependent coefficient, and results in the V_{M2-} decreasing to $V_{dc} - Nv_{D-}$. In this situation, the green-thick dc load line will move to the left, as a red line, leading the operation point q_{20} moving left to q_{2-} while $v_{DS} = V_{DS2-}$, and while the MOSFET operates in the triode region and its drain current is $i_{DS} = I_{2-}$; correspondingly, when the string N -LED current decreases, reducing its luminance, even its voltage V_D is slightly increasing. Accordingly, it may happen to push the operation point from the saturation region into the triode region, due to the increase of N -LED's voltage in a lower temperature situation.

(3) Ambient Temperature rising to $T = T_+$

If the temperature increases to T_+ from T_0 , where $T_+ > T_0$, the green-thick dc load line will move right, as a blue line, due to V_{M2+} increasing to $V_{dc} - Nv_{D+}$, which leads the operation point q_{20} to move right to q_{2+} on the flat v_{GS2-} characteristic curve. Accordingly, the $i_{DS} = I_{2+} \approx I_{20}$ and even the v_{DS} increases to V_{DS2+} ; meanwhile, the string N -LED current is $i_D = I_{2+} \approx I_{20}$, which keeps its luminance at almost the same value as that produced at I_2 .

(4) Bias Situation for the MOSFET with Constant V_{dc} Supply for $T_+ > T_0 > T_-$

In order to explain the drain-to-source voltage of the MOSFET for $T_+ > T_0 > T_-$ under a constant voltage V_{dc} supply, a voltage sum $v = Nv_D + i_{DS}R_s$ is introduced in Figure 3b. The voltage v , as the dark brown line, clearly displays the variation of v_{DS} between saturation and the triode regions, due to the temperature effect, where $v_{DS} = V_{dc} - v$.

2.3. Dimming with a Constant Voltage Supply to LCR

When using a LCR loaded with one string LED, with a constant supply of V_{dc} , for example, in the dimming process, the operation point of the MOSFET under different drives v_{GS} 's will change dramatically, since the voltage drop v_R on the source resistor R_s will vary far more than the voltage Nv_D . In this description, three kinds of gate voltages v_{GS} 's are explored, to dim the string N -LED. As mentioned previously, the operation of LCR is initially placed at point q_2 under normal temperature T_0 , as shown in Figure 4, in which the N -LED current $i_D = I_{D2}$ under the MOSFET is driven by v_{GS2} . If the gate voltage changes from v_{GS2} to v_{GS1} while $v_{GS1} < v_{GS2}$, the operation point q_2 will move to

point q_1 on the flat v_{GS1} -characteristic curve, since the voltage Nv_D will decrease due to the decrease of i_D , lowering the LED luminous output. On the other hand, if the gate voltage varies from v_{GS2} to v_{GS3} for example, as well as $v_{GS3} > v_{GS2}$, the voltage $v_{DS} = V_{DS3}$ will move left, to point q_3 on the triode region of the v_{GS3} -characteristic curve. In this instance, the drain current i_{DS} will increase to I_{D3} since the voltage drop on R_s and Nv_D will increase, leading to the decrease of v_{DS} . Therefore, although an increase of the N -LED current $i_D = I_{D3}$ will raise the luminance, the luminance change may not be proportional to the dimming level, disturbing its uniform distribution variation.

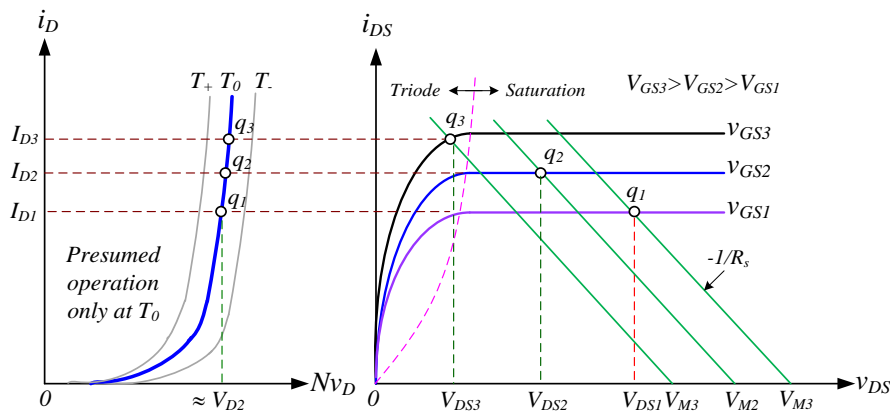


Figure 4. Bias situations for MOSFET and a single string LED during dimming process at $T = T_0$, where the LCR is supplied with constant V_{dc} .

3. Variable Voltage Regulator for LCRs to Balance the String LED Currents

3.1. VV_{dc} Synthesized to Clamp Low-Dropout v_{DS} in the MOSFET

As mentioned in Figures 3 and 4, for a LCR with constant voltage V_{dc} supply, the drain-to-source voltage v_{DS} is not only dependent on the forward voltage of the string LED, but is also subject to the voltage drop v_R of the source resistor R_s . Accordingly, the v_R will increase, due to the increase of i_{DS} ; the v_{DS} may fall dramatically to enter into the triode region of the MOSFET. On the contrary, the v_{DS} will be located far away from the triode region, due to the reducing i_{DS} , and the operation point will move right. Here, it will be sustained on the flat v_{GS} -characteristic curve, on which the drain current i_{DS} will remain almost constant in a wide variation of v_{DS} , resulting in a N -LED luminance output which is almost the same. In order to remedy the issue due to a constant voltage V_{dc} supply, a constant low-dropout v_{DS} is initially specified as V_Q , close to the boundary of triode region, but on the flat portion of the v_{GS} -characteristic curve. Subsequently, all drain voltages at points M , v_{Mk} , are only supplied by a variable dc supply VV_{dck} from a variable voltage regulator (VVR), in which the low dropout V_Q is involved, i.e.,

$$\begin{aligned} v_{Mk} &= VV_{dck} - Nv_{Dk} \\ &= V_Q + v_{Rk} \end{aligned} \quad (12)$$

where the footnote “ k ” denotes the k th operation point, and:

$$v_{Rk} = i_{DSk}R_s \quad (13)$$

Then, the output voltage VV_{dc} of VVR can be estimated as:

$$\begin{aligned} VV_{dck} &= Nv_{Dk} + V_Q + i_{DSk}R_s \\ &= Nv_{Dk} + v_{Mk} \end{aligned} \quad (14)$$

where the V_Q is a constant low voltage placed close to the boundary of the triode region, but in the saturation region, as shown in Figure 5a, i.e.,

$$V_Q = VV_{dc} - v_k \quad (15)$$

$$\equiv \text{constant}$$

where the sum of the voltage v_k is given by:

$$v_k = Nv_{Dk} + i_{DSk}R_s \quad (16)$$

Accordingly, the VV_{dc} can then be synthesized from (14), including Nv_D , $i_{DS}R_s$, and the specified low-dropout V_Q , as shown in Figure 5b. In Figure 5a, the supply v_{Mk} for different operation points under constant V_Q , can be easily found in (12). Remarkably, with a variable supply VV_{dc} , the LCR is able to keep the MOSFET operating at the specified V_Q under different v_{GS} 's, which are the corresponding dimming levels. In addition, with the low-dropout V_Q , the MOSFET can only dissipate low conduction loss, and the string N -LED can emit luminance, proportional to the dimming levels.

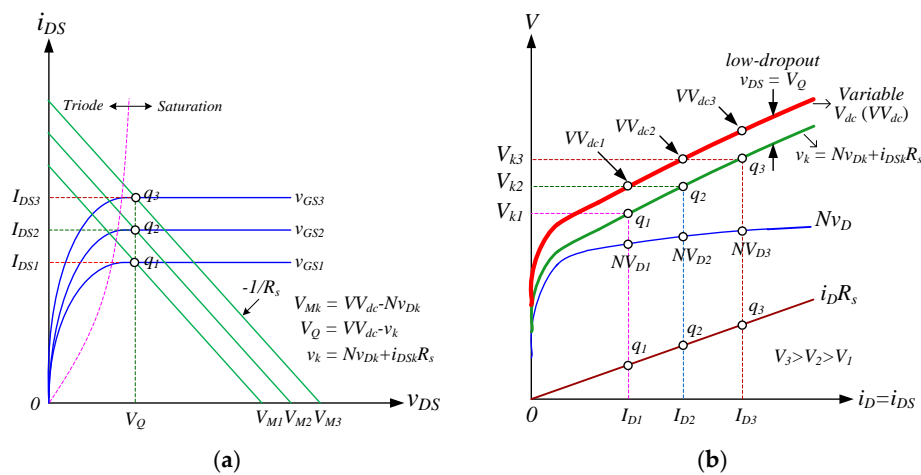


Figure 5. (a) Predicted bias situation of MOSFET with a constant low dropout v_{DS} , where the LCR is supplied with a variable V_{dc} ; (b) Bias construction for the synthesized VV_{dc} with low-dropout v_{DS} .

3.2. Dimming for Multiple-String N -LEDs

For dimming multiple-string N -LEDs, multiple identical i_{DS} - v_{DS} planes, as shown in Figure 6, are simultaneously controlled by multiple LCRs with varying v_{GS} values, in which all v_{DS} 's are then placed at a constant low-dropout $v_{DS} = V_Q$. For the convenience of analysis, all components, including MOSFETs, OPAs, LEDs, and source resistor R_s , are assumed to be identical in an array of integrated circuits (ICs), in which only one VV_{dc} , as shown in Figure 5b, is supplied in the planes of Figure 6. For the ease of analysis, two i_{DS} - v_{DS} planes are taken as being the same as each other, for example, in which V_{Q1} and V_{Q2} are the low-dropout voltages. Since the two MOSFETs are identical, the two operation points are almost the same, leading to the two string LEDs having the same currents. However, once there is a deviation from v_{DS} , at least one of the MOSFET's v_{DS} should be maintained at the specified V_Q , leaving the rest of v_{DS} 's as being greater than V_Q , but still remaining on the same flat v_{GS} -characteristic curve; on which both of the drain currents of the MOSFETs in this example are almost the same, but are different for the v_{DS} . Thus, the two string N -LEDs can still have the same currents, and thus emit the same luminance. This control theme is to be extended to the current balance of multiple string N -LEDs.

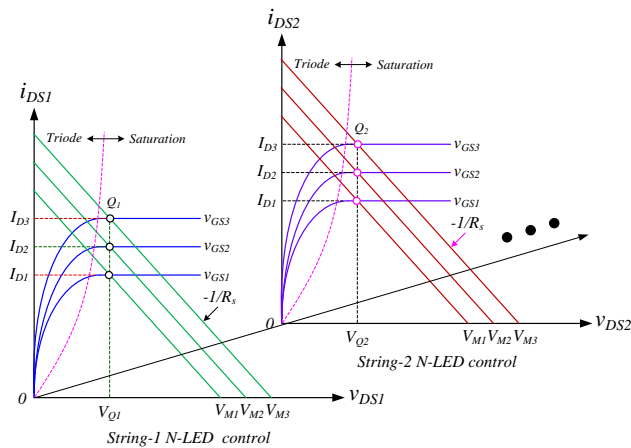


Figure 6. Current balance control for multiple-string N -LEDs using multiple identical i_{DS} - v_{DS} planes, where all of the MOSFETs and LCRs are assumed to be identical with VV_{dc} supply.

3.3. Master and Slave Control for Current Balance of Multiple string N -LEDs

In this study, using an array of ICs to acquire identical MOSFETs for serving multiple-string N -LED control, is vital work. The circuit scheme for the multiple LCRs respectively loaded with one string N -LED, is outlined in Figure 7, in which the master and slave controls for the current balance are built. Since the devices and components, in practice, can be selected as almost identical to one another, the current balance between the adjacent string LEDs can then be realized as predictions. The control reference is preset at the master LCR and wires together with the other slave LCRs. The VV_{dc} of VVR is basically synthesized by the loop parameters of the master LCR, as per Figure 5b, including the v_{DS} of the MOSFET, v_R on source R_S , Nv_D on the N -LED, and the specified low voltage dropout V_Q . To implement the VVR, a reference voltage $(V_Q + V_k)_{ref}$ is initially preset, where V_k depends on the state of the gate drive v_{GS} . After comparing the instantly detected voltage $(v_k + v_{DS})$ with the $(V_Q + V_k)_{ref}$ in the master loop, the synthesized VV_{dc} is then adapted to supply all multiple string LEDs through the LCRs, and results in the same currents for adjacent LEDs, while holding all v_{DS} 's positions greater than the lowest V_Q . Once the control is finished in the master LCR, all slave LCRs with the updated supply VV_{dc} , can mirror the master drain current on their flat v_{GS} -characteristic curves in the i_{DS} - v_{DS} planes, and then all slave string LED currents are almost the same as one another.

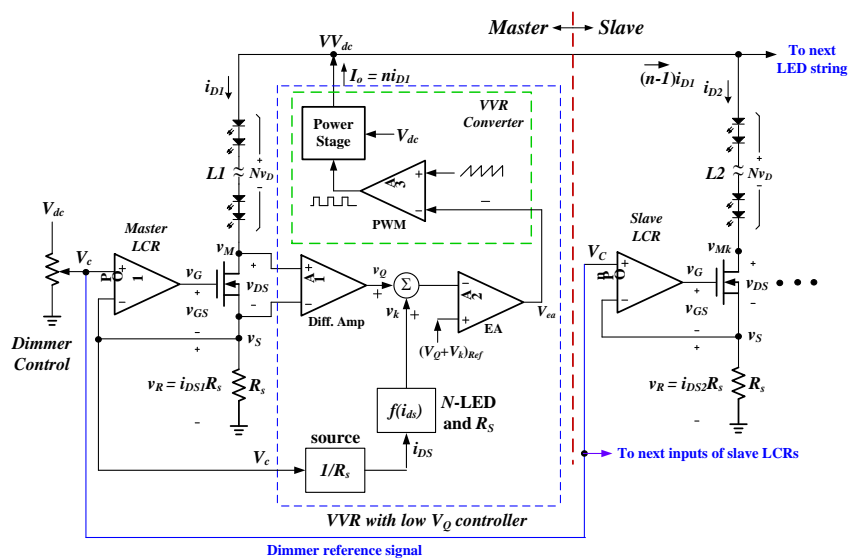


Figure 7. Configuration of master and slave control for the current balance of multiple string N -LED.

3.4. Digitizing the VVR Controller

Figure 8 shows the digital control architecture used to build the VVR, in which the controller is executed by Microchip dsPIC33FJ06GS202, according to the idea theme in Figure 5b. The mentioned three parameters, v_{DS} , v_R , and Nv_D , detected from the master LCR are respectively sampled and held before the digitizing process. After combining them, a $v_k + v_{DS}$ through D/A is obtained, to compare with the reference $(V_Q + V_k)_{ref}$ at the error amplifier (EA). The error signal from the EA will then guide the VVR to provide an updated VV_{dc} for supplying the master and slave LCRs. This digitizing process makes the VV_{dc} produced from VVR more accurate and stable against the parameter variations mentioned previously.

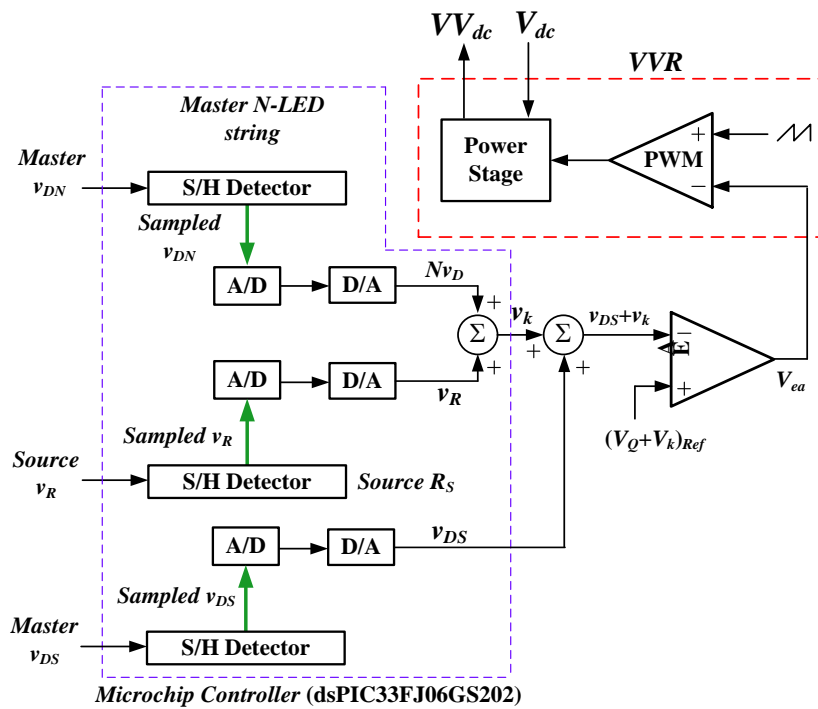


Figure 8. The algorithm to implement VVR for supplying the LCRs, executed by Microchip dsPIC33FJ06GS202 with reference to Figure 5b.

4. Design and Experiment

To verify the proposed control theme, a scaled-down simple layout of 5×6 LEDs are arranged with five string LEDs connected in parallel, in which each string has six LEDs in series. Five LCRs are employed to drive the five string LEDs, respectively, in which MOSFET IRF110 is used as the current regulator in LCR, and the LED EHP-C04/UT01-P01/TR with a rated power of 1 W is adopted. The operational amplifier TL074 with a slew rate of $13 \text{ V}/\mu\text{s}$ is used as a comparator. The power LED has a conductance (i_D/v_D) of approximately $0.42 \text{ mA}/\text{mV}$. The transconductance (i_{DS}/v_{GS}) of the MOSFET is about $2.97 \text{ mA}/\text{mV}$ under an i_{DS} varying from 0 mA to 350 mA; correspondingly, v_{GS} varies from 3.72 V to 4.5 V. The low-dropout $v_{DS} = V_Q$, is 1.5 V, specified at $i_{DS} \approx 200 \text{ mA}$. The circuit schemes for the experiment are as in Figures 7 and 8, in which the digital controller for synthesizing the VVR is as per the loop parameters of the master LCR, with reference to the estimation profile in Figure 5b. In Figure 7, the v_{DS} is instantly detected by the differential amplifier (A1) and is controlled at a low dropout V_Q . The voltage $v_k = f(i_{DSk})$ in (16) is a function of the k th current i_{DSk} detected from a source voltage (v_R), in which the voltage v_k is the summation of v_R and Nv_D , where the footnote “ k ” is used to denote the position of the operation point driven by v_{GSk} . The v_Q and v_k are merged at the inverting input of the error amplifier (A2) and compared with a specified reference

voltage $(V_Q + V_k)_{ref}$. After comparing the error output V_{ea} from A2 with a reference sawtooth at the PWM controller (A3), an updated variable voltage VV_{dc} from the VVR is acquired through the loop regulation in the master LCR. With the VV_{dc} , the v_{DS} 's in the five string LCRs can then be kept at a low dropout V_Q on the five flat v_{GS} -characteristic curves, respectively. A source resistor $R_s = 12 \Omega$ which is, estimated for the current sensor is used, the VVR is supplied by a dc source $V_{dc} = 35 V$, and the dimmer control is implemented by a precision variable resistor. The digitizing controller, as shown in Figure 8, is implemented by Microchip dsPIC33FJ06GS202, in which three parameters, including v_{D5} , v_R , and v_{DS} , detected from the control loop of the master LCR, are sampled and held for digitizing. Through D/A conversion, the voltage v_k is acquired. After merging the v_k and v_{DS} to compare with the reference $(V_Q + V_k)_{ref}$ at the error amplifier (EA), the updated VV_{dc} from the VVR to supply the five LED strings, is achieved. Consequently, the self-feedback in the control loop of the master LCR for keeping all slave v_{DS} 's at low dropout is always valid, and indeed the updated VV_{dc} is able to achieve the current balance in the multiple LED strings.

4.1. Experiment for a Single String 6-LED

The experiment to evaluate the characteristics of a LCR to drive a single string 6-LED and their relative parameters during v_{GS} changes, is shown in Figure 9. The synthesis voltage VV_{dc} composed of $v_{DN} = Nv_D$, V_R , and v_{DS} , under the v_{GS} control, is displayed in Figure 9a, in which all of the parameters measured meet the estimations with an acceptably low dropout voltage. The experiment shows that v_{DS} varies at around 1.5 V, from 1.77 V to 1.38 V, in all five MOSFETs; correspondingly, their v_{GS} varies from 3.72 V to 4.46 V.

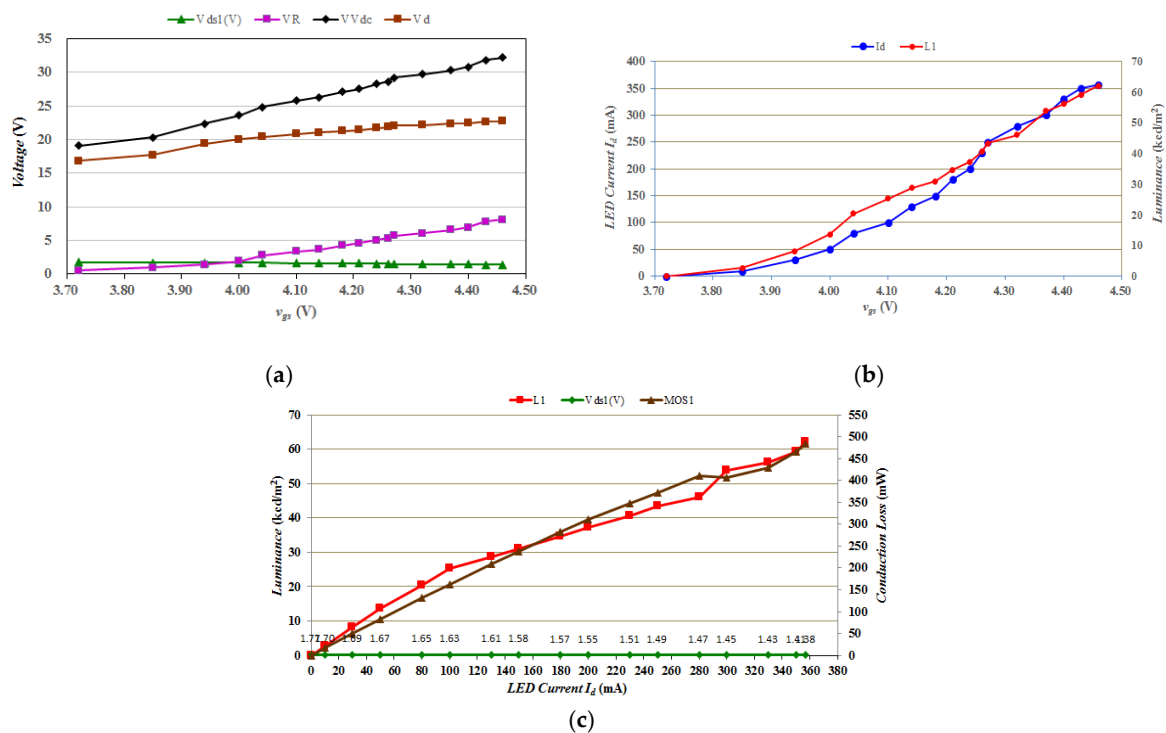


Figure 9. Characteristics of the master LCR loaded with a single string 6-LED in dimming process by v_{GS} controlled: (a) The synthesized VV_{dc} composed of a specified $V_{D51} \equiv V_Q \cong 1.5 V$, v_R , and $v_{D5} \equiv 5v_D$; (b) LED current i_D versus v_{GS} ; (c) LED luminance with respect to conduction loss of MOSFET during dimming.

The LED luminance, with respect to the LED current i_D under the v_{GS} control, is shown in Figure 9b, in which each string 6-LED can emit a luminance from 0 to 62.1 kcd/m²; correspondingly, the string LED current i_D varies from 0 to 357 mA. The string LED luminance is measured vertically, facing the LED display at a distance of 50 cm, by using a luminance-meter type BM-910 TOPCON with a high accuracy. The string LED luminance and the conduction loss in MOSFET are measured in Figure 9c. It is clearly seen that the maximum conduction loss in the MOSFET is only 492 mW at $i_{DS} = 357$ mA, due to a low dropout of $v_{DS} \approx 1.38$ V, which actually benefits the MOSFET, dissipating the low conduction loss.

4.2. Experiment for the Multiple String 6-LEDs

In this experiment, the master and the four slave LCRs are supplied by the same VV_{dc} , and all of the controls are wired with the same dimmer signal. The VV_{dc} is controlled by the loop of the master LCR. With the VV_{dc} , each slave LCR can self-regulate the MOSFET's v_{DS} to stay at the low dropout V_Q , even at place higher than V_Q toward right-side, where the drain current can always mirror the master current during the dimmer control.

The variations of the five v_{DS} 's, with respect to each string's LED current, are shown in Figure 10a, in which the highest v_{DS} is 1.78 V and the lowest v_{DS} is 1.37 V, and all are located on the flat v_{GS} -characteristic curves. With reference to $v_{DS} = V_Q = 1.5$ V, the deviation Δv_{DS} above V_Q is 0.28 V and below V_Q is 0.13 V, in which the low deviation is still on the flat v_{GS} -characteristic curve in the saturation region of MOSFET. The luminance's distribution of the 5-group LED strings during the LED current change is displayed in Figure 10b, in which the adjacent luminance values between 6-LED strings are almost the same during a wide dimmer range. In this measurement, the maximum luminance deviation, of about ± 0.45 kcd/m², occurs at the highest luminance of 62.7 kcd/m² (where $i_{DS} = 357$ mA) and the minimum deviation of about ± 0.01 kcd/m² at the lowest 2.65 kcd/m² (where $i_{DS} = 10$ mA). The measured luminance can be expected to be uniform if the proposed 5×6 LED layout is equipped in a panel display. This experiment successfully demonstrates the current balance strategy for the multiple string LED; particularly, the control theme, which is easy to implement by using simple LCRs with a microchip control. The experimental setup of a scale-down 5×6 LED display is shown in Figure 11.

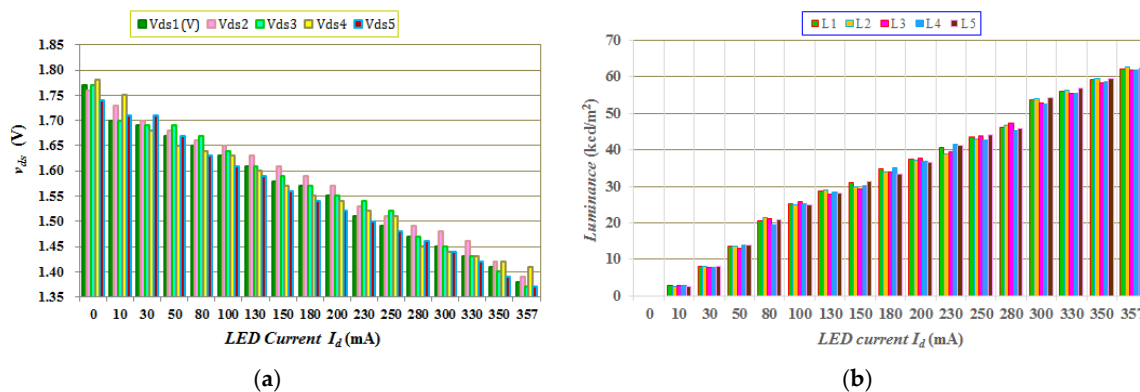


Figure 10. The measurements of the five string 6-LEDs connected in parallel during dimming process: (a) Drain-to-source voltage v_{DS} 's; (b) Luminance's emitted from the five string 6-LED, all measures are group-displayed with respect to the string LED currents.

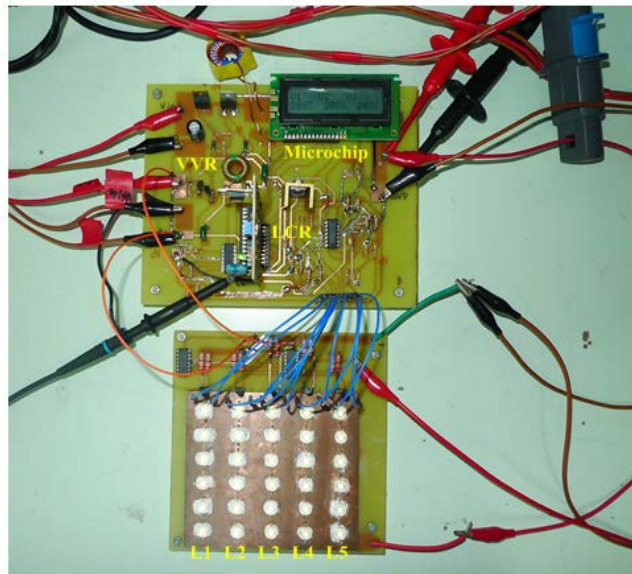


Figure 11. Experimental setup of a scale-down 5×6 LED display arranged by five string 6-LED in parallel connection, which can produce a uniform luminous output from 0 kcd/m^2 to 62.7 kcd/m^2 for the entire dimming range.

5. Conclusions

In this paper, the synthesized VVR successfully achieves a low dropout v_{DS} for all MOSFETs in the LCRs, and allows their operation points to remain on the flat v_{GS} -characteristic curves, on which all of the drain currents are almost the same and actually attain the balance of the multiple string LED currents. In addition, the experiment evidenced that the control strategy is feasible in practice. All measurements, including the current balance behavior, low dropout voltage deviation, and the distribution of luminance between the adjacent string LEDs etc., all meet the estimations. Consequently, the cost-effective LCRs with the proposed control theme can actually achieve the current balance in multiple string LEDs, and it would be suitable to extend their use to a large-scale display that requires multiple string LEDs.

Acknowledgments: This work was supported by the Ministry of Science and Technology under Award Number MOST 105-2221-E-415-014. The authors would like to thank Ssu-Wei Peng and Jhih-Ting Cheng for providing the experimental measurements.

Author Contributions: Hung-I Hsieh conceived and designed the experiments; Hao Wang performed the experiments; Hung-I Hsieh analyzed the data; Hung-I Hsieh contributed materials and analysis tools; Hung-I Hsieh wrote the paper.

Conflicts of Interest: The authors declare no conflict of interest.

References

- Swanson, D.F.; Criscione, M. LED Driver Circuit and Method. U.S. Patent 6,362,578 B1, 26 March 2002.
- Burgyan, L.; Prinz, F. High Efficiency LED Driver. U.S. Patent 6,690,146 B2, 10 February 2004.
- Otake, T. Switching Constant-Current Power Supply System. U.S. Patent 7,235,899 B2, 26 June 2007.
- Narra, P.; Zinger, D.S. An Effective LED Dimming Approach. In Proceedings of the IEEE Industry Applications Conference, Seattle, WA, USA, 3–7 October 2004.
- Nishikawa, M.; Ishizuka, Y.; Matsuo, H.; Shigematsu, K. An LED Drive Circuit with Constant-Output-Current Control and Constant-Luminance Control. In Proceedings of the International Telecommunications Energy Conference (INTELEC), Providence, RI, USA, 10–14 September 2006.

6. Van der Broeck, H.; Sauerlander, G.; Wendt, M. Power Driver Topologies and Control Schemes for LEDs. In Proceedings of the IEEE Applied Power Electronics Conference and Exposition (APEC), Anaheim, CA, USA, 25 February–1 March 2007.
7. Garcia, J.; Calleja, A.J.; Corominas, E.L.; Gacio, D.; Campa, L.; Díaz, R.E. Integrated driver for power LEDs. In Proceedings of the IEEE Industrial Electronics Conference (IECON), Glendale, AZ, USA, 7–10 November 2010.
8. Chen, H.; Zhang, Y.; Ma, D. A SIMO Parallel-String Driver IC for Dimmable LED Backlighting With Local Bus Voltage Optimization and Single Time-Shared Regulation Loop. *IEEE Trans. Power Electron.* **2012**, *27*, 452–462. [[CrossRef](#)]
9. Li, S.N.; Zhong, W.X.; Chen, W.; Hui, S.Y.R. Novel Self-Configurable Current-Mirror Techniques for Reducing Current Imbalance in Parallel Light-Emitting Diode (LED) Strings. *IEEE Trans. Power Electron.* **2012**, *27*, 2153–2162. [[CrossRef](#)]
10. Choi, S.; Kim, T. Symmetric Current-Balancing Circuit for LED Backlight with Dimming. *IEEE Trans. Ind. Electron.* **2012**, *59*, 1698–1707. [[CrossRef](#)]
11. Choma, J. Temperature Stable Voltage Controlled Current Source. *IEEE Trans. Circuits Syst. I Fundam. Theory Appl.* **1994**, *41*, 405–411. [[CrossRef](#)]
12. Doshi, M.; Zane, R. Digital Architecture for Driving Large LED Arrays with Dynamic Bus Voltage Regulation and Phase Shifted PWM. In Proceedings of the IEEE Applied Power Electronics Conference and Exposition (APEC), Anaheim, CA, USA, 25 February–1 March 2007.
13. Chiu, H.J.; Lo, Y.K.; Chen, J.T.; Cheng, S.J.; Lin, C.Y.; Mou, S.C. A High-Efficiency Dimmable LED Driver for Low-Power Lighting Application. *IEEE Trans. Ind. Electron.* **2010**, *57*, 735–743. [[CrossRef](#)]
14. Chiu, H.J.; Cheng, S.J. LED Backlight Driving System for Large-Scale LCD Panels. *IEEE Trans. Ind. Electron.* **2007**, *54*, 2751–2760. [[CrossRef](#)]
15. Oh, I.H. An Analysis of Current Accuracies in Peak and Hysteretic Current Controlled Power LED Drivers. In Proceedings of the IEEE Applied Power Electronics Conference and Exposition (APEC), Austin, TX, USA, 24–28 February 2008.
16. Hu, Y.; Jovanovic, M.M. LED Driver with Self-Adaptive Drive Voltage. *IEEE Trans. Power Electron.* **2008**, *23*, 3116–3125. [[CrossRef](#)]
17. Hu, Q.; Zane, R. LED Driver Circuit with Series-Input-Connected Converter Cells Operating in Continuous Conduction Mode. *IEEE Trans. Power Electron.* **2008**, *25*, 574–582.
18. Zhang, R.; Chung, H.S.H. Paralleled LED Strings—An Overview of Current Balancing Techniques. *IEEE Ind. Electron. Mag.* **2015**, *9*, 17–23. [[CrossRef](#)]
19. Sedra, A.S.; Smith, K.C. *Microelectronic Circuits*, 7th ed.; Oxford University Press: New York, NY, USA, 2016; pp. 174–230.
20. Lin, Y.L.; Chiu, H.J.; Lo, Y.K.; Leng, C.M. Light-Emitting Diode Driver with a Combined Energy Transfer Inductor for Current Balancing Control. *IET Power Electron.* **2015**, *8*, 1834–1843. [[CrossRef](#)]
21. Gacio, D.; Alonso, J.M.; Garcia, J.; Garcia-Llera, D.; Cardesin, J. Study on Passive Self-Equalization of Parallel-Connected LED Strings. *IEEE Trans. Ind. Appl.* **2015**, *51*, 2536–2543. [[CrossRef](#)]
22. Ye, Y.; Cheng, K.W.E.; Lin, J.; Wang, D. Single-Switch Multichannel Current-Balancing LED Drive Circuits Based on Optimized SC Techniques. *IEEE Ind. Electron.* **2015**, *62*, 4761–4768. [[CrossRef](#)]
23. Wu, X.; Hu, C.; Zhang, J.; Qian, Z. Analysis and Design Considerations of LLC Resonant Multioutput DC/DC LED Driver with Charge Balancing and Exchanging of Secondary Series Resonant Capacitors. *IEEE Trans. Power Electron.* **2015**, *30*, 780–789. [[CrossRef](#)]
24. Chen, X.; Huang, D.; Li, Q.; Lee, F.C. Multichannel LED Driver with CLL Resonant Converter. *IEEE J. Emerg. Sel. Top. Power Electron.* **2015**, *3*, 589–598. [[CrossRef](#)]
25. Hwu, K.I.; Jiang, W.Z. Nonisolated Two-Channel LED Driver with Automatic Current Balance and Zero-Voltage Switching. *IEEE Trans. Power Electron.* **2016**, *31*, 8359–8370. [[CrossRef](#)]
26. Hsieh, H.I.; Peng, S.W.; Cheng, J.T. Low-Dropout Voltage Regulator for Stabilizing LEDs Drives in Dimmable Group Current Sinks. In Proceedings of the IEEE Applied Power Electronics Conference and Exposition (APEC), Fort Worth, TX, USA, 6–11 March 2011.

